Lycium Barbarum Polysaccharides Protect Retina in rd1 Mice During Photoreceptor Degeneration

Feng Liu,[1] Jia Zhang,[1] Zongqin Xiang,[1] Di Xu,[1] Kwok-Fai So,[1–3] Noga Vardi,[4] and Ying Xu[1–3]

[1]Guangdong-Hongkong-Macau Institute of CNS Regeneration, Ministry of Education CNS Regeneration Collaborative Joint Laboratory, Jinan University, Guangzhou, China
[2]Changsha Academician Expert Workstation, Aier Eye Hospital Group, Changsha, China
[3]Co-Innovation Center of Neuroregeneration, Nantong University, Jiangsu, China
[4]Department of Neuroscience, University of Pennsylvania, Philadelphia, Pennsylvania, United States

Correspondence: Ying Xu, GHM Institute of CNS Regeneration, Jinan University, 601 West Huangpu Avenue, Guangzhou 510632, Guangdong, China; xuying@jnu.edu.cn.

FL and JZ contributed equally to the work presented here and should therefore be regarded as equivalent authors.

Submitted: August 28, 2017
Accepted: December 18, 2017

Citation: Liu F, Zhang J, Xiang Z, et al. Lycium barbarum polysaccharides protect retina in rd1 mice during photoreceptor degeneration. *Invest Ophthalmol Vis Sci*. 2018;59:597–611. https://doi.org/10.1167/iovs.17-22881

Purpose. As an active component in wolfberry, lycium barbarum polysaccharides (LBP) are capable of protecting retinal neurons in several animal disease models. Here, we asked whether LBP rescues the retinal morphology and function in rd1 mouse, a photoreceptor fast-degenerating animal model of retinitis pigmentosa, and in particular focused on LBP's effects on the function of retinal ganglion cells (RGCs) during photoreceptor degeneration.

Methods. An equal volume of LBP or control vehicle was daily intraperitoneal (i.p.) injected in rd1 mice from postnatal day 4 (P4) to P14, P20, or P24 when photoreceptors completely degenerate. Immunostaining, electroretinogram (ERG), visual behavior tests and multielectrode array (MEA) recordings were assessed to determine the structure and function of the treated retina.

Results. LBP treatment greatly promoted photoreceptor survival, enhanced ERG responses, and improved visual behaviors in rd1 mice. MEA data showed that LBP treatment in general decreased the abnormally high spontaneous spiking that occurs in rd1 mice, and increased the percentage of light-responsive RGCs as well as their light-evoked response, light sensitivity, signal-to-noise ratio, and response speed. Interestingly, LBP treatment affected ON and OFF responses differently.

Conclusions. LBP improves retinal morphology and function in rd1 mice, and delays the functional decay of RGCs during photoreceptor degeneration. This is the first study that has examined in detail the effects of LBP on RGC responses. Our data suggest that LBP may help extend the effective time window before more invasive RP therapeutic approaches such as retinoprosthesis are applied.

Keywords: retinal ganglion cells, photoreceptor degeneration, multi-electrode array, light responses, neuroprotection

Retinitis pigmentosa (RP) is a hereditary retinal disease caused by the progressively sequential loss of rod and cone photoreceptors, ultimately leading to complete blindness.[1] Many approaches have been applied to either slow down photoreceptor degeneration or replace diseased cells, including antioxidant treatment, manipulating sigma 1 receptor signaling,[2] genetic or stem cell therapy, retinal prosthesis, and so on.[3–7] Nevertheless, the success of any of these interventions depends considerably on the functional integrity of retinal ganglion cells (RGCs), whose axons transmit the visual information to higher brain centers. Thus, it is critical to maintain their normal physiology, or at least delay the functional impairment of RGCs so as to allow the application of those photoreceptor restorative therapies.

There are over 10 types of RGCs in the retina, and each transmits different types of visual information to the brain. Based on their responses to light onset (ON) or offset (OFF), RGCs can be classified into ON, OFF, or ON-OFF subsets. With the loss of photoreceptor inputs, the light responses of RGCs diminish at different rates for various RGC types.[8–10] Generally, in animal models of RP (e.g., rd1 and rd10 mice, or RCS and P23H rats), ON RGCs lose their responses before OFF RGCs.[9,11–13] Another common finding in RGCs of RP animal models is the increase of oscillatory spontaneous activity,[8,9] which greatly reduces the efficiency and capacity of visual information processing.[14] Furthermore, the oscillatory activity is type-dependent in rd1 mice and P23H rats, and predominant in OFF RGCs of the latter.[13,14] Such variability of light responses and oscillatory spontaneous spiking among various RGC types implicates an advantage of targeting ON and OFF pathways separately when designing strategies for retinal protection or replacement, especially those involving a direct electrical[15] or optical stimulation.[16]

Lycium barbarum polysaccharides (LBP) as an active component of wolfberry consist of six monosaccharides (galactose, glucose, rhamnose, arabinose, mannose, and xylose) and antioxidants. LBP possesses a wide range of biological activities, such as antioxidation, anti-inflammation, antiapoptosis, as well as neuroprotection observed in several animal models for retinal diseases, including glaucoma, ischemia, optic nerve transection, and RP.[17–20] Previously, Wang et al.[20] demonstrated an improvement of the retinal structure and

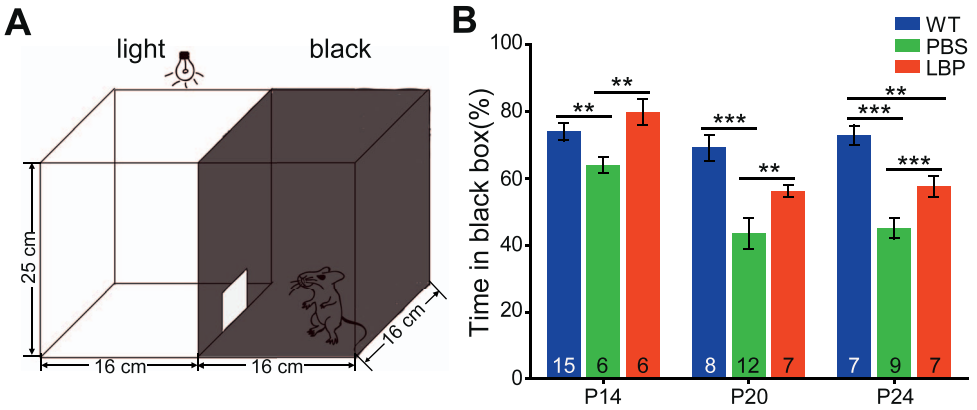

Figure 1. LBP treatment improves the visual performance of rd1 mice. (**A**) Illustration of the black/white transition box for visual behavior tests. (**B**) Percentage of time in the *black chamber* (relative to total time in the box) for different animal groups across ages. WT mice with normal vision preferred to stay in darkness, but rd1 mice with gradual loss of light perception had no such preference. LBP treatment significantly increased the duration of rd1 mice in the *black chamber*. The numbers within the *bars* represent the numbers of animals tested. $^{**}P < 0.01$ and $^{***}P < 0.001$ by one-way ANOVA.

function by LBP application in the rd10 model of RP. However, whether this Wolfberry component can also exert a protection to the rd1 mouse model characterized by faster photoreceptor degeneration remains unclear. In addition, it is uncertain whether the protective effect is RGC type dependent.

In the current study, we addressed the above questions by investigating the effects of LBP on retinal neurons in rd1 mice. Our data showed that LBP not only slowed down photoreceptor degeneration and increased ERG responses, but also improved visual behaviors. In the meantime, LBP treatment reduced the abnormally high spontaneous firing of RGCs, and enhanced their response and sensitivity to light stimulation. Interestingly, the protective effects in RGCs were differential between ON and OFF responses.

Methods

Animals

Wild-type (WT; C57BL/6N) and C3H/HeJ (rd1) mice were obtained from Guangdong Medical Lab Animal Center and Model Animal Research Center (MARC) of Nanjing University, respectively. Animals of either sex used in the experiments were kept under standard laboratory conditions with 12-hour/12-hour light–dark cycles, and were supplied with food and water ad libitum. All procedures were performed according to the ARVO Statement for the Use of Animals in Ophthalmic and Vision Research and approved by Competent Ethics Committees at Jinan University. All efforts were made to minimize the number of animals used and their suffering.

Pretreatment With Lycium Barbarum Polysaccharides (LBP)

LBP was extracted by Shanghai Institute of Material Medica as previously described[21] (Supplemental Figs. 1A, 1B). Briefly, the aqueous extract of dried fruits of L. barbarum Lynn (Ningxia, China) was prepared sequentially by decoloration and delipidation in alcohol, and boiling in distilled water. The extract was then freeze-dried into powder for storage. For experimental use, the LBP solution was freshly prepared by dissolving the powder in PBS (0.01 M, pH 7.4). The rd1 littermates were randomly divided into two groups receiving either LBP (10-mg/kg body weight)[22] or control vehicle treatment. LBP or PBS was intraperitoneally (i.p.) injected into rd1 mice once per day, starting at postnatal day (P) 4 (a few days before the onset of rod photoreceptor degeneration at P8)[23] and lasting until P14 (the early stage of photoreceptor degeneration), P20 (the middle stage), or P24 (the late stage) when photoreceptors completely degenerate.

Behavioral Assessment

Visual behavior tests were conducted on mice of different ages using a black-white box (custom made by Metronet Technology Ltd., Hong Kong SAR, China; Fig. 1A), as previously described.[24] The box consists of a dark chamber ($16 \times 16 \times 25$ cm, illuminated with infrared light) and a white chamber of the same size (illuminated with bright white light). An aperture (10×12 cm) on the wall that separates the black and white chambers allows mice to travel freely from one chamber to the other. Two cameras, individually installed in each chamber, captured mouse activity and were connected to a recorder and a monitor (Noldus Information Technology BV, Wageningen, the Netherlands). A mouse was placed in the middle of the white chamber at the start of a trial, and removed from the box 5 minutes later; the time spent in the black chamber was measured with EthoVision XT 8.0 software (Noldus Information Technology BV).

Electroretinogram (ERG)

After behavioral tests, mice were dark adapted for 3 hours[25,26] and the in vivo retinal function was determined with the RETIscan system (Roland Consult, Wiesband, Germany) as described by us before.[27] Briefly, mice were anesthetized with tribromoethanol (0.14 ml/10g body weight of 1.25%) and put on a heated platform (37°C) under dim red light. Pupils were dilated with phenylephrine HCl (0.5%) and tropicamide (0.5%). ERG was recorded with gold-plated wire loop electrodes contacting the corneal surface as the active electrode. Stainless steel needle electrodes were inserted into the skin near the eye and into the tail to serve as the reference and ground leads, respectively. Animals were first stimulated with a green flash with an intensity of 3.0 cd·s/m^2 under dark adaptation. Thereafter, they were light adapted for 5 minutes with a bright green background (20 cd/m^2), and recorded for the photopic response to green flashes of 10.0 cd·s/m^2. ERG data were collected by the amplifier of the RETI-scan system at a sampling rate of 2 kHz, and subsequently analyzed with RETIport software (Roland Consult) after applying the 50-Hz

Investigative Ophthalmology & Visual Science

low-pass filtering. The a-wave amplitude was measured from the baseline to the first negative peak, and the b-wave amplitude was measured from the a-wave trough to the subsequent largest positive peak. For each animal, the better response of the two eyes was selected as the data point. When no clear light-induced ERG response was observed (i.e., no peak response beyond the baseline following light onset), the animal was regarded to be nonresponsive to light.

Immunocytochemistry

After ERG recording, animals were killed by anesthetic overdose with tribromoethanol. Both eyes were enucleated and fixed in 4% paraformaldehyde (PFA) for 30 minutes at 4°C. Thereafter, eyes were rinsed in PBS, cryoprotected overnight at 4°C in phosphate buffer (0.1 M, pH 7.4) containing 30% sucrose, and embedded in the optimal cutting temperature compound (OCT; Tissue Tek, Torrance, CA, USA). Retinas were cryosectioned through the optic disk longitudinally at a thickness of 10 μm, and slices were mounted on glass slides for future processing.

Before staining, the slides were washed three times with 0.1% Triton X-100 in PBS (PBST), and then treated with 0.3% PBST containing 3% normal donkey serum and 1% bovine serum albumin for 1 hour. Retinal sections were subsequently probed with the primary antibodies overnight at 4°C, followed by the corresponding secondary antibodies for 1 hour at room temperature. 4′,6-diamidino-2-phenylindole (DAPI; 1:1000; Electron Microcopy Sciences, Hatfield, PA, USA) was used to counterstain nuclei. The primary antibodies used included rabbit anti-PKCα (right, 1:20,000, Sigma-Aldrich Corp., St. Louis, MO, USA), rabbit-anti-cone arrestin (1:500, a gift from Cheryl Craft), and rabbit-anti-CtBP2 (1:1000; Synaptic Systems, Goettingen, Germany) for staining rod bipolar cells, cones, and synaptic ribbons, respectively. The secondary antibodies were donkey-anti-mouse and donkey-anti-rabbit IgG conjugated to Alexa 488 or 594 (1:1000; Invitrogen, Carlsbad, CA, USA).

Image Acquisition and Analysis

Fluorescent images from retinal sections were captured using Zeiss LSM700 confocal microscope (Carl Zeiss, Oberkochen, Germany). Because the photoreceptor degeneration in rd1 mice follows a center-to-periphery gradient, we compared structures at the same eccentricity (1.0–1.3 mm away from the center of the optic disk). To estimate the survival of photoreceptors, the number of DAPI-positive cells in the outer nuclear layer (ONL), where the photoreceptor somas are located, was counted by ImageJ software (http://imagej.nih.gov/ij/; provided in the public domain by the National Institutes of Health, Bethesda, MD, USA). To measure the length of cone outer segments (OS) or axons, a line was drawn along the axis of each structure stained by cone arrestin, and its length was measured accordingly. To analyze the shape of PKCα-positive cells, the longest diameter of cell bodies and the longest diameter perpendicular to the height were taken as the height and the width, respectively; the height/weight ratio was calculated as the "soma aspect ratio," where a larger soma aspect ratio indicates a more oval shape. The number of PKCα-positive cells was counted by ImageJ. For each retina, counts from three to six slices (image size: 320 × 320 μm) were averaged to provide a data point, and these data points of all retinas from the same group were again averaged to get the mean value.

Multielectrode Array (MEA) Recording and Data Collection

Mice were dark adapted for 2 to 3 hours before euthanization by anesthetic overdose with tribromoethanol under dim red light. After the careful removal of the cornea, lens, and vitreous body from the enucleated eye, the retina was isolated and transferred to the oxygenated AMES solution containing Ames' Medium (8.8 g/L, #A1420; Sigma-Aldrich Corp.) and $NaHCO_3$ (1.9 g/L, #792519; Sigma-Aldrich Corp.). The solution was bubbled with 95% O_2 and 5% CO_2 to maintain a pH of 7.3 to 7.4. A whole piece of retina was cut into quarters, and the middle region from each quarter with an area of approximately 2×2 mm^2 was dissected and flattened on the 8×8 MEA array (electrode diameter: 20 μm; interspace: 100 μm; P210A; Alpha MED Scientific, Inc., Osaka, Japan) (Supplemental Fig. 2). The retina was pressed down on the array by a platinum ring to obtain a close contact between the ganglion cells and the electrodes. The MEA array with the retina was transferred to the recording stage, connected to the amplifier (MED64 amplifier; Alpha MED Scientific, Inc.), and superfused continuously with the oxygenated AMES solution at a rate of 4 to 5 mL/min at 31°C to 33°C. At least 40 minutes were required to stabilize the action potential amplitude, number of cells recorded, spontaneous firing rate, and consistency of light-evoked responses. Unless otherwise specified, data were acquired within 2 hours after mounting the retina.

The MEA system with MED64 amplifier and Mobius software (Alpha MED Scientific, Inc.) were used for recording and filtering spike trains from each electrode in the array. Extracellular spikes were bandpass filtered between 100 and 5000 Hz, digitized at a rate of 20 kHz and subsequently analyzed off line. After recording, the position of the tissue on the array was verified under a dissecting microscope and a bright field image was recorded with a digital camera (Mshot Image Analysis System; MC16, Guangzhou, China).

Visual Stimulation

After dark adaptation in a light-tight enclosure, retinas were stimulated with a white organic light-emitting diode (LEDWE-15; Thorlabs, Newton, NJ, USA) with the stimulation intensity and duration controlled by the main amplifier (MED64; Alpha MED Scientific, Inc.). The full-field flash covered the spot region of a 2-mm diameter, and was focused onto the photoreceptor layer of the retina. The flash stimulation intensities used were 1.5×10^4, 1.2×10^5, 1.6×10^6, 6.3×10^6, and 3.6×10^7 photons/μm^2/s, which were calibrated via a commercial radiometer (ILT1400-A; International Light Technologies, Peabody, MA, USA). For each intensity, the full-field flash consisted of a 2-seconds light ON, followed by an 8-seconds light OFF (0 photons/μm^2/s), and was repeated 30 times. The stimuli were able to evoke a reliable response and allow the separation of ON and OFF responses in individual ganglion cells.

Spike Sorting and Data Analysis

Typically, each MEA electrode recorded the spikes from one to four RGCs. We applied spike sorting to separate the responses from each individual cell with Offline Sorter software (Offline Sorter; Plexon, Dallas, TX, USA). The response threshold was set to 4.5 times above the SD of the noise level. Only RGC somatic spikes with a bi-phasic spike waveform (excluding axonal spikes with a triphasic waveform) were used, as described before.[28] Principal component analysis (PCA) of spike waveforms was used for sorting spikes in individual cells, and only those with interspike intervals (ISI) >1 msec were included in the analysis. Sorted spike timestamps were then exported to Spike2 (Version 8; CED, Cambridge, England), Matlab (Version 2013b; MathWorks, Natick, MA, USA), and R software (Version 3.3.0; The R Project for Statistical Computing, Vienna, Austria), where the customized programs trans-

formed the waveforms containing multiunit activities into spike trains of a single RGC. Thereafter, peristimulus time histograms (PSTHs) and raster plots of individual cells with a 10-msec bin width were generated from its responses to the full-field flash stimulation. To further analyze spike patterns or classify RGCs and compare activities of the responding RGCs within the same class, the following calculations are performed:

First, to determine whether a RGC responded to ON or OFF stimuli, we computed the response dominant index (RDI) using the following equation (Equation 1)[29,30]:

$$\mathrm{RDI} = \frac{R_{\mathrm{ON}} - R_{\mathrm{OFF}}}{R_{\mathrm{ON}} + R_{\mathrm{OFF}}}, \quad (1)$$

where R_{ON} and R_{OFF} are, respectively, the average spike rate during the first 2 seconds of ON or OFF portions of the stimulus, with the basal spiking rate in darkness subtracted. This equation gives a value of RDI between −1 and 1. Cells with a RDI smaller than −0.6 or larger than 0.6 were defined as OFF-dominating or ON-dominating RGCs, respectively; cells with a RDI between −0.6 and 0.6 were defined as ON-OFF RGCs.

To evaluate the percentage of visually responsive RGCs, the visually responsive index (VRI) was calculated in Equation 2:

$$\mathrm{VRI} = \frac{R_{\mathrm{average}}}{R_{\mathrm{spontaneous}}}, \quad (2)$$

where R_{average} is defined as the average firing frequency during the first 0.2 seconds after light onset (for ON response) or offset (for OFF response), or the mean of ON and OFF responses (for ON-OFF response), and $R_{\mathrm{spontaneous}}$ is quantified as the average spike rate during 2 seconds before the light stimulation. RGCs with a VRI <3 were categorized as a nonresponsive population.

To assess the visual information transfer efficiency in the retina,[31] the signal-to-noise ratio (SNR) was calculated as shown in Equation 3:

$$\mathrm{SNR} = \frac{\mu_{\mathrm{signal+noise}} - \mu_{\mathrm{noise}}}{\mu_{\mathrm{noise}}}, \quad (3)$$

where $\mu_{\mathrm{signal+noise}}$ is the mean firing rate in the ON or OFF response within 2 seconds after light onset or offest, and μ_{noise} is the mean firing rate during darkness within 2 seconds before light onset (i.e., spontaneous). As some RGCs fired only in response to a flash but not darkness (zero in μ_{noise}), their SNR was immeasurably high, and thus excluded for further analysis.

To determine the light sensitivity of different types of RGCs, the peak firing rate of each cell was plotted as a function of light intensity and then fitted with the Hill equation as follows[32]:

$$R = \frac{R_{\max} \mathrm{I}^N}{\mathrm{I}^N + \sigma^N}, \quad (4)$$

where R is the measured response, $R_{\max}$ represents the maximum response, I indicates stimulus intensity, σ indicates the intensity that evokes a half-maximal response (thus, representing the light sensitivity), and N is the Hill coefficient. Only cells with a good fit ($N > 0.8$) were included and the σ values were compared among different groups.

We also analyzed the time-to-peak value of light responses, that is, the interval between the onset and offset of light stimulus and the appearance of the peak firing rate. The time-to-peak value of ON-OFF RGCs is the average of the two.

To assess the deterioration of light responses in rd1 cells, we introduced the relative response ratio by normalizing the peak responses in rd1 cells to the mean of peak responses in WT control cells at the same age. Likewise, to determine the protective effects of LBP on the ON and OFF responses of RGCs, we calculated the LBP/PBS ratio as the peak light responses in LBP-treated rd1 cells to the mean of peak responses in PBS-treated rd1 cells at the same age. We further defined the cumulative distribution of LBP/PBS ratios as the percentage of cells below a certain LBP/PBS value.

Statistical Analysis

One- or two-way ANOVA were applied to compare the results from LBP-treated rd1 mice, untreated rd1 mice, and WT mice with SPSS software (Version 17.0; IBM, Chicago, IL, USA) or GraphPad software (Prism 5.0; San Diego, CA, USA), depending on the number of variable factors. The unpaired Student's *t*-test was used for comparing two groups, and one-way ANOVA with correction for repeated measures for comparing the intensity curves. Kruskal-Wallis tests were performed for comparing the cumulative distribution curves, and χ^2 analyses for comparing the percentages of cell types among different groups across ages. For all statistical tests, we hypothesized that the data from three groups (nontreated rd1, LBP-treated rd1, and WT mice) were similar. This hypothesis would be rejected if $P < 0.05$; the differences would be considered significant if $P < 0.05$ or highly significant if $P < 0.01$. Unless otherwise specified, the data are presented as means ± SE.

Results

LBP Treatment Improves the Visual Performance of rd1 Mice

We examined the protective effects of LBP on the visual pathway of rd1 mice using a range of tests for visual behavior, retinal light response, retinal morphology, and RGC electrophysiologic property (Supplemental Fig. 1C). In rd1 mice, the death of rods begins at approximately P8 and is nearly completed by P21.[23] Therefore, we i.p.-injected LBP (10-mg/kg body weight) into mice daily from P4 until their euthanization. The animals were tested at the time of early (P14), middle (P20), and late stages (P24) of retinal degeneration, as reported before.[33,34]

For the behavioral test, we used the black-white box (Fig. 1A) and estimated the tendency of mice to stay in darkness. A WT mouse with normal vision, that is placed in the center of a lighted chamber will enter the dark chamber and spend most of the time there. As photoreceptors degenerate, rd1 mice gradually lose the ability to detect illuminance, and thus their stay in the black chamber becomes much shorter than that of WT counterparts. In our study, time in black and white chambers was comparable for rd1 mice at P20. Across all ages, LBP-treated rd1 mice spent a significantly longer duration in darkness than PBS-treated controls ($P < 0.01$ by one-way ANOVA; Fig. 1B). Following LBP treatment, the percentage of total time that animals stayed in the black chamber was extended from 64% to 80% ($P < 0.01$ for PBS versus LBP) at P14, from 44% to 56% ($P < 0.01$) at P20, and from 45% to 58% ($P < 0.001$) at P24. Thus, LBP treatment improves the visual performance in rd1 mice.

LBP Treatment Improves Retinal Light Responses in rd1 Mice

Next, we determined the retinal function by ERG. Retinal neurons in WT mice (blue lines) at all ages responded well to light flashes under both dark-adapted (Fig. 2A) and light-adapted (photopic) conditions (Figs. 2D, 2F). Under dark adaptation, the light responses in rd1 mice dramatically

Investigative Ophthalmology & Visual Science

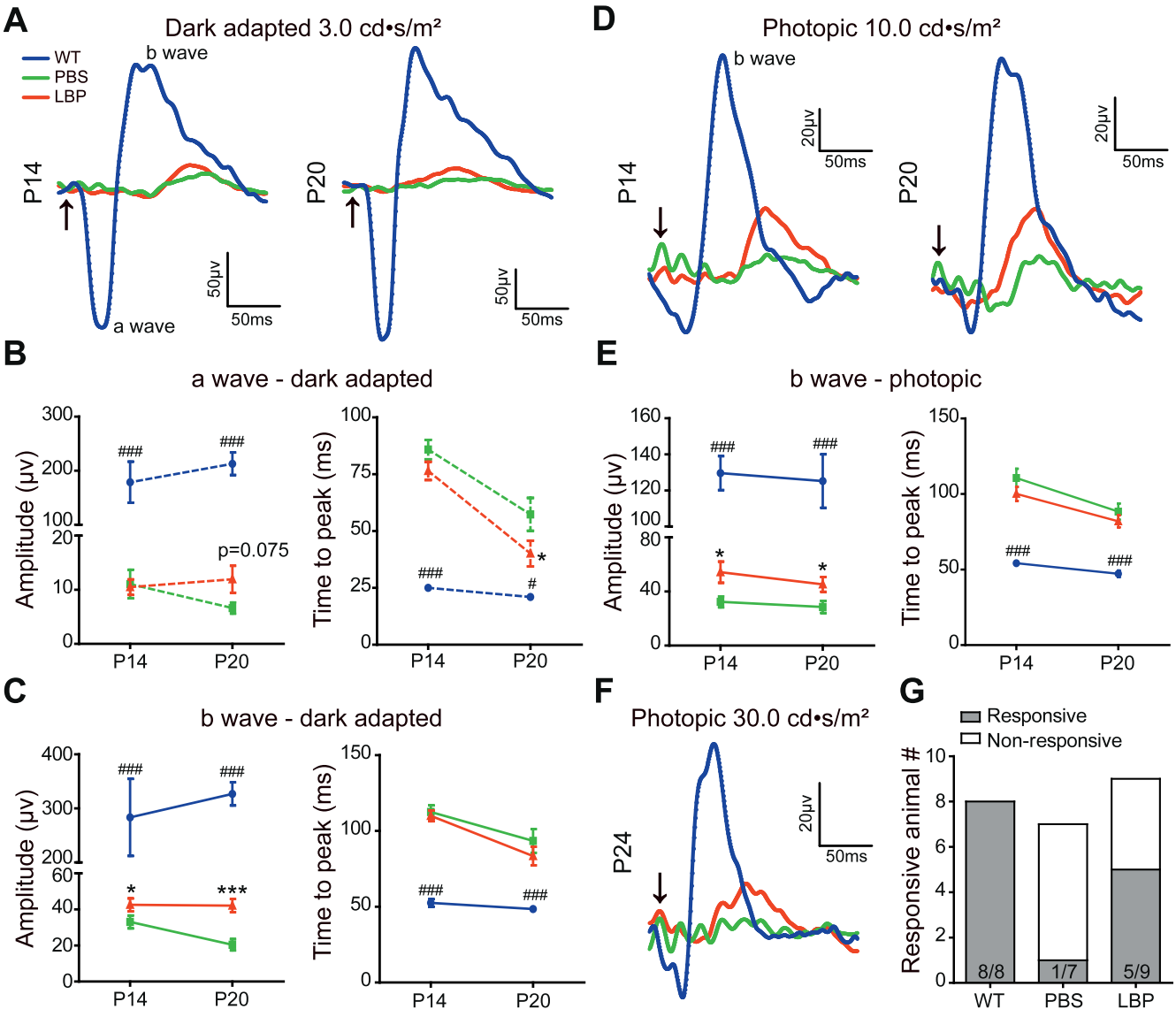

Figure 2. LBP treatment improves retinal light responses in rd1 mice. (**A**) Average ERG traces to a 3.0 cd·s/m^2 flash under dark adaptation of WT (*blue*), or rd1 mouse receiving PBS (*green*), or LBP treatment (*red*) at P14 (*left panel*) and P20 (*right panel*). *Arrows* indicate the flash onset. (**B**, **C**) The average peak amplitude and time to peak of a- (**B**) and b-waves (**C**) in different groups under dark adaptation at P14 and P20. (**D**) Average ERG traces to a 10.0 cd·s/m^2 flash under light adaptation (photopic) of different animals at P14 (*left panel*) and P20 (*right panel*). (**E**) The average peak amplitude and time to peak of photopic b-waves in different groups at P14 and P20. (**F**) Average ERG traces to a 30.0 cd·s/m^2 flash under light adaptation of different animals at P24. (**G**) The numbers of mice with (responsive) and without light responses (nonresponsive) in different groups at P24. ERG responses were decreased in rd1 mice compared with that in WT controls, which were further restored by LBP treatment. The animals included in different groups were: 6 (P14, P20) and 8 (P24) WT; 11 (P14), 9 (P20) and 7 (P24) PBS-treated rd1; 12 (P14), 10 (P20) and 9 (P24) LBP-treated rd1 mice. For P24, the numbers within the *bars* represent the number of responsive mice over that of all mice tested. $^{*}P < 0.05$, $^{***}P < 0.001$ versus untreated mice; and $^{\#}P < 0.05$, $^{\#\#\#}P < 0.001$ versus LBP-treated rd1 mice by one-way ANOVA.

decreased (green traces) and became undetected by P24 (data not shown). At P14, LBP treatment significantly increased the b-wave amplitude from 33 ± 3.6 to 42 ± 3.6 μV ($P < 0.05$ for PBS versus LBP by Student's *t*-test; Fig. 2C), and at P20 it increased from 20 ± 3.1 to 42 ± 3.6 μV ($P < 0.001$; Fig. 2C). No apparent effect of LBP on the scotopic a-wave amplitudes was observed (Fig. 2B). As for the time to peak, LBP-treated mice responded faster, but the difference was not significant.

Under photopic conditions, the a-wave was too small to measure accurately; hence, only the b-wave amplitude was compared. As shown in Fig. 2E, LBP treatment significantly elevated the photopic b-wave amplitude when compared with the PBS-treated group, from 32 ± 4.0 to 54 ± 7.9 μV ($P < 0.05$) at P14 and from 29 ± 4.5 to 45 ± 5.5 μV ($P < 0.05$) at P20. At P24, very few PBS-treated rd1 mice responded to flash stimuli even with a strong flash intensity of 30 cd·s/m^2 (Fig. 2F); therefore, we calculated the percentage of responsive animals instead. The results showed that LBP substantially raised the percentage of light-responsive rd1 animals from 14% to 56% (Fig. 2G); the time to peak was shorter, but with no significant difference (Fig. 2E). In contrast to the similar amplitude of the a-wave, that of the b-wave reflecting light responses of ON-bipolar cells that depend on the input from photoreceptors was increased, suggesting an overall enhancement of photoreceptor responses. Notably, although LBP treatment improved the ERG responses in rd1 mice, such a change was much smaller than that in WT counterparts.

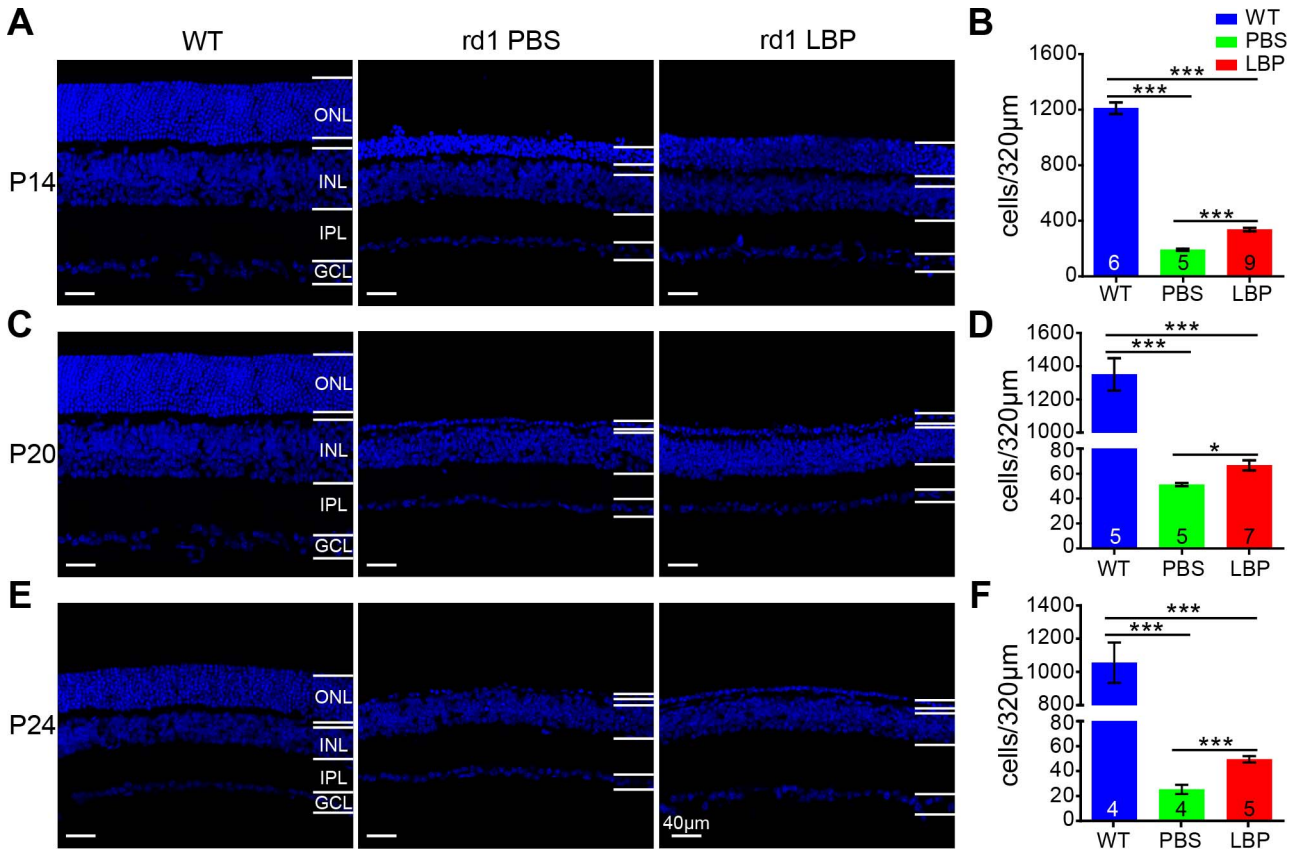

Figure 3. LBP treatment promotes the survival of photoreceptors in rd1 mice. (**A**, **C**, **E**) Images of retinal sections stained with DAPI for WT (*left panel*), and PBS- (*middle*) or LBP-treated (*right*) rd1 mice at P14 (**A**), P20 (**C**), and P24 (**E**). (**B**, **D**, **F**) Quantification of the photoreceptor number per image (a length of 320 μm) at P14 (**B**), P20 (**D**), and P24 (**F**). Treatment with LBP in rd1 mouse greatly increased the survival of photoreceptors. The numbers within the *bars* represent the number of animals tested. $^{*}P < 0.05$, $^{***}P < 0.001$ by one-way ANOVA or independent-sample *t*-tests (for P20 and P24). INL, inner nuclear layer; GCL, ganglion cell layer.

LBP Improves Retinal Morphology in rd1 Retina

Next, we tested the effect of LBP on retinal morphology by assessing the survival of photoreceptors identified as DAPI-positive cells in the ONL where their somas are located. By P14, the number of DAPI-positive cells per image (a length of 320 μm) in PBS-treated rd1 retinas was dramatically decreased to 15.8% of WT controls ($P < 0.001$), which was significantly reversed to 27.8% following LBP administration ($P < 0.001$; Figs. 3A, 3B). As displayed in Figure 3C, only one tier of somas was left in the ONL for both PBS- and LBP-treated rd1 mice at P20 in the middle stage of photoreceptor degeneration; nonetheless, the number of surviving cells was much larger in the LBP-treated group (67 ± 4.1 cells/image) than in the PBS-treated control group (51 ± 1.2 cells/image; $P < 0.05$; Fig. 3D). Photoreceptors in rd1 retinas at P24, the late stage of degeneration, almost disappeared in the PBS-treated group (25 ± 3.8 cells/image), whereas one tier of somas still remained following LBP application (49 ± 2.6 cells/image; $P < 0.01$; Figs. 3E, 3F). It is noteworthy that although LBP evidently raised the survival of photoreceptors, the number of photoreceptors still considerably decreased compared with that in WT mice.

When photoreceptors die, their terminals degenerate. In order to test the degree of preservation at the synaptic regions, we quantified the number of synaptic ribbons by staining with an antibody against CtBP2. In the WT retina, CtBP2 staining in the outer plexiform layer (OPL) showed numerous ribbons: some were of a horseshoe shape indicating their location in rod terminals, and others were organized in a row as in cone terminals (Fig. 4A). In contrast, in the rd1 retina, hardly any ribbons were observed even at P14, suggesting the loss of terminals was prior to the loss of somas for rods. LBP treatment significantly increased the number of ribbons in OPL ($P < 0.05$ for PBS versus LBP; Fig. 4D).

Considering the great improvement in cone-driven response measured by ERG, we next quantified the number of cones. In WT mice, the cone outer segments (COS) were intensely stained for the specific marker arrestin, with the somas and their long axons observable in the ONL (Fig. 4B, left panel), whereas most of the COS diminished and the axons became shorter in rd1 mice (Fig. 4B, middle panel). In the LBP-treated group, the number of cone somas increased significantly (Fig. 4F; $P < 0.05$ versus PBS group). The length of the COS was slightly greater in LBP-treated mice, but the difference was not significant ($P > 0.5$; Figs. 4B, 4E). Moreover, the cone axons were significantly longer than that of the PBS-treated group ($P < 0.05$, Fig. 4G), consistent with the observation of a thicker ONL.

To assess morphologic changes beyond photoreceptors, we also evaluated the density and morphology of rod bipolar cells using the PKCα antibody. In WT mice, rod bipolar cells clearly exhibited fusiform somas and lush dendrites (Fig. 4C, left panel). In rd1 mice, the somas of rod bipolar cells became round and dendrites started to retract (Fig. 4C, middle panel). At P14, the morphology of rod bipolar cells after LBP

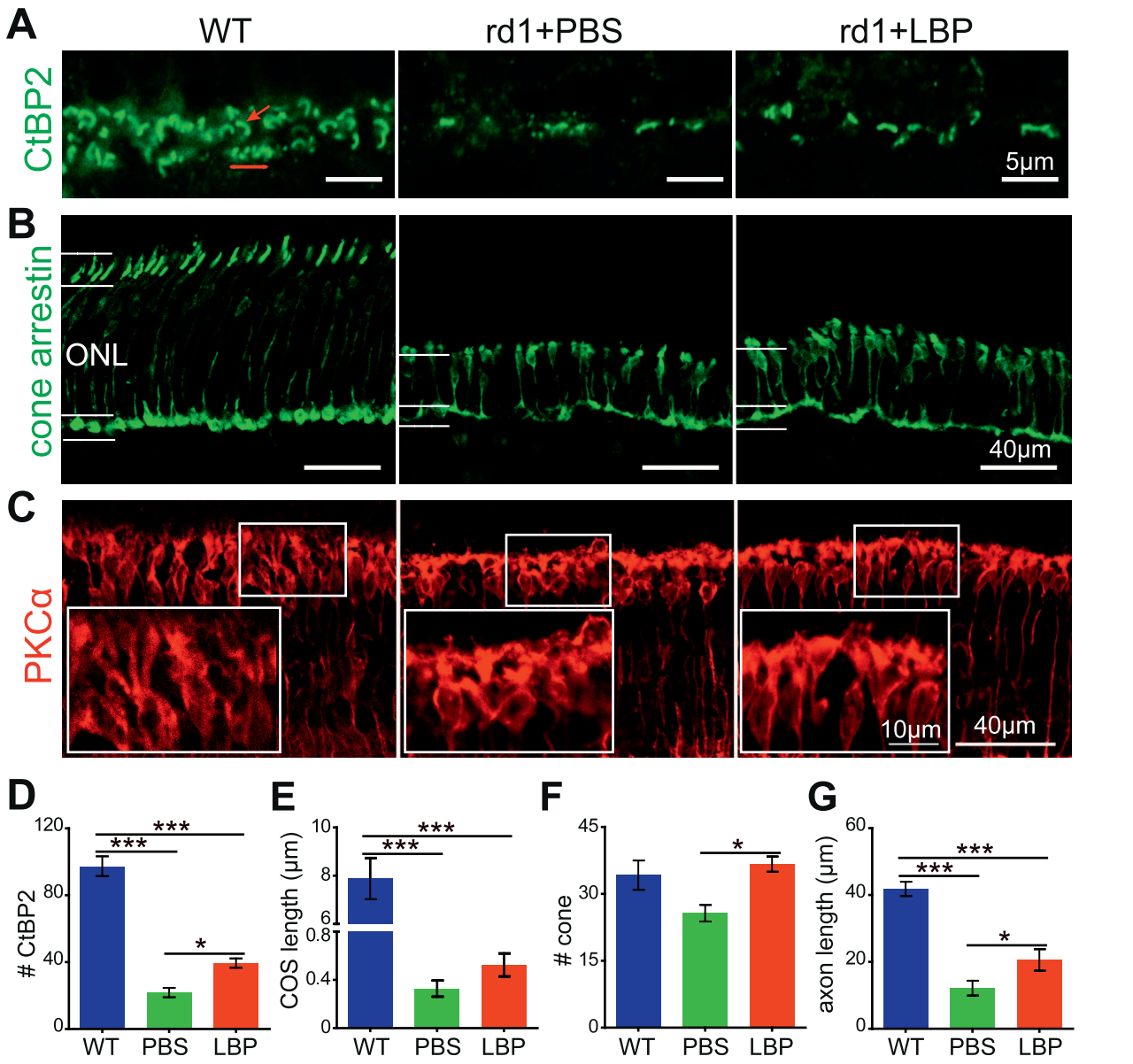

Figure 4. LBP treatment partially preserves the morphology of ribbons, cones, and rod bipolar cells in rd1 mice. (**A–C**) Images of CtBP2 (*green*) (**A**), cone arrestin (*green*) (**B**), and PKCα (*red*) (**C**) staining in the OPL layer in retinal slices from different animal groups at P14. The *red arrow* points to a rod ribbon with a *horseshoe shape* and the *red line* shows the ribbons in the cone terminal. *Boxed areas* in (**C**) were enlarged to show the somas and dendrites of rod bipolar cells. (**D–G**) Quantification of the number of ribbons per 100-μm length (**D**), the length of COS (**E**), the number of cones per 320-μm length (**F**), and the length of cone axons (**G**) for different groups. LBP treatment restored the number of ribbons and cones in rd1 mice, and improved the structure of cones and rod bipolar cells. The numbers within the *bars* represent the number of animals tested. $^{*}P < 0.05$, $^{**}P < 0.01$, $^{***}P < 0.001$ by one-way ANOVA.

treatment appeared essentially normal, with more branching dendrites and less round somas than those of PBS-treated rd1 counterparts (Fig. 4C, right panel). The soma aspect ratio, measured as the height/width of the cell soma, was significantly smaller in rd1 mice (1.7 ± 0.06, $n = 3$) as compared with WT controls (2.7 ± 0.14, $n = 3$, $P < 0.01$); in LBP-treated mice, this ratio was significantly higher (2.4 ± 0.10, $n = 3$, $P < 0.01$) than the PBS-treated group. No difference was observed with regard to the number of rod bipolar cells among the three animal groups (data not shown). Together, our data indicate that LBP treatment not only improves photoreceptor survival, but also partially restores the normal morphology of rod bipolar cells.

LBP Treatment Increases the Light Responses of RGCs

As LBP treatment significantly improved the morphology and function of outer retinal neurons, we expected functional improvement of inner retinal neurons, as well. This is particularly important because the recording from ganglion cells provides a more comprehensive assessment of the effects of degenerative processes at the output from the eye to the brain. To investigate the detailed functional changes of RGCs, the MEA recording was applied (Supplemental Figs. 2A, 2B).

We initially tested how many RGCs remained light responsive during photoreceptor degeneration at the designat-

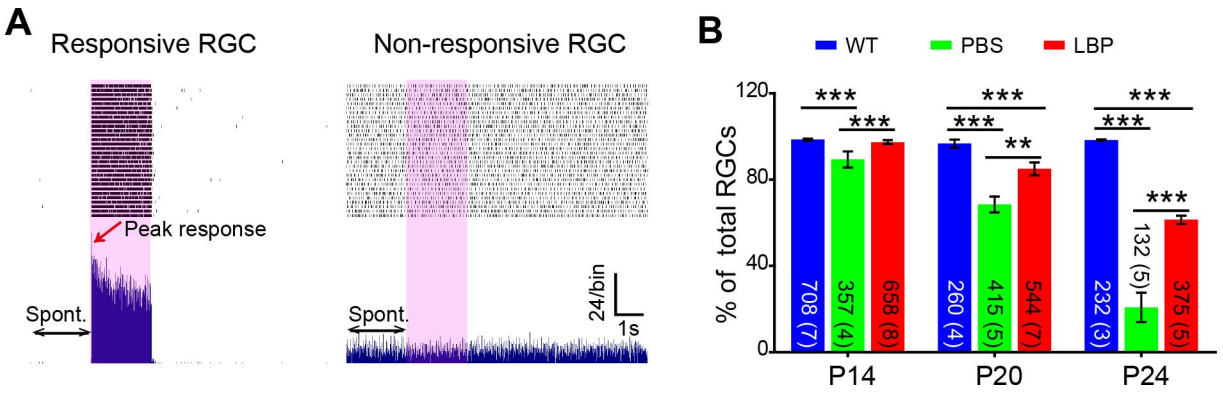

Figure 5. LBP treatment increases the percentage of light responsive RGCs in rd1 mice. (**A**) Representative activity of a light-responsive (*left panel*) or nonresponsive (*right panel*) RGC in the LBP-treated rd1 retina. Each panel shows raster plots (*top*) from 30 repeats of a 10-second recording from a single cell and the corresponding PSTH (*bottom*). The 2-second light stimuli are indicated by *pink boxes*. *Double arrows* indicate the 2-second prestimulation interval when the spontaneous firing (Spont.) rate was measured. The *red arrow* points to the peak response. (**B**) The percentage of visually responsive RGCs for different animal groups across ages. This percentage greatly decreased in untreated rd1 mice (*green*) at all ages, which was significantly reversed following LBP treatment (*red*). The numbers within the *bars* represent the number of responsive cells recorded from retinas, with number of retinas shown in parenthesis. $^{**}P < 0.01$, $^{***}P < 0.001$ by χ^2 analysis.

ed time points. Examples of light-responsive and nonresponsive cells are shown in Figure 5A. In WT mice, this percentage (relative to the whole cell population that exhibited the spontaneous and/or light-evoked spiking) constantly remained close to 100% during physiological development. However, in rd1 mice, the percentage of responsive cells dropped drastically from 89.3% ± 3.8% at P14 to 20.8% ± 6.8% at P24 ($P < 0.001$, χ^2 analysis). Treatment with LBP significantly raised the percentage of responsive cells at all ages, with the largest difference observed at P24 (PBS-treated: 21%, LBP-treated: 61%, $P < 0.01$; Fig. 5B). Accordingly, our results demonstrate that LBP treatment greatly increases the response rate of RGCs in rd1 mice.

Next, we tested whether LBP treatment affected the spontaneous firing of RGCs in rd1 mice, which is abnormally high and compromises the reliability of signal transduction.[9,35] The spontaneous firing of all the recorded RGCs (including both light-responsive and nonresponsive cells) greatly increased as rd1 mice aged (Fig. 6A), and was reduced by LBP administration at P14 (PBS-treated: 7.2 ± 0.3, $n = 719$; LBP-treated: 5.3 ± 0.2, $n = 678$) and at P20 (PBS-treated: 19.7 ± 0.6, $n = 603$; LBP-treated: 17.5 ± 0.5, $n = 640$; $P < 0.01$ by two-way ANOVA). At P24, LBP had little effect (PBS-treated: 23.3 ± 0.6, $n = 637$; LBP-treated: 22.5 ± 0.7, $n = 616$; $P > 0.05$).

Lastly, we compared the light responses of all RGCs to full-field flashes among different groups. Across all ages, LBP treatment clearly enhanced the light-evoked peak responses compared with PBS vehicle ($P < 0.001$ by two-way ANOVA; Fig. 6B). Following LBP treatment, the increase was observed not only in the response magnitude, but also in the mean firing rates within 2 seconds after light onset or offset (Fig. 6C).

As LBP treatment lowered spontaneous firing and enhanced light responses of rd1 RGCs, we speculated that LBP would augment the SNR, which is the average light-evoked response divided by the average spontaneous firing.[11] In rd1 mice, application of LBP increased the SNR from 13% to 55% compared with that of WT controls at P14 ($P < 0.001$ for PBS-treated rd1 versus LBP-treated rd1 groups by one-way ANOVA) and from 10% to 17% at P20 ($P < 0.05$; Fig. 6D); however, at P24, the SNR was barely improved after LBP treatment.

Another useful index for responsiveness and efficiency of coding is the time to peak response after light onset or offset.[26] As photoreceptors degenerated, the time to peak in rd1 mice was prolonged; at each time point specified, this index in rd1 mice was greater than that in WT counterparts (Fig. 6E). Treatment with LBP significantly shortened the time to peak from 0.14 ± 0.003 seconds in untreated rd1 RGCs to 0.12 ± 0.002 seconds in LBP-treated group at P14, from 0.16 ± 0.010 to 0.10 ± 0.003 seconds at P20, and from 0.24 ± 0.028 to 0.14 ± 0.008 seconds at P24 ($P < 0.01$ by two-way ANOVA; Fig. 6E). Collectively, the results obtained from various experiments uniformly suggest that LBP greatly promotes RGCs' responses to light stimuli in rd1 mice.

LBP Treatment Increases Light Sensitivity of RGCs in rd1 at P20

The above-mentioned experiments assessing the light responses of RGCs were exclusively performed using flashes at a saturating intensity (7.6 log photons/μm^2/s). To further test how LBP treatment affected light response and to calculate light sensitivity, we stimulated the RGCs with flashes over a range of intensities. For this analysis, we classified the RGCs into three classes based on their responses to light ON (transient and sustained), OFF (transient and sustained), and ON-OFF (transient and sustained; Supplemental Fig. 2C). Examples of an ON RGC's response to flashes with increasing intensities in WT, untreated rd1, and LBP-treated rd1 mice are shown in Fig. 7A. The firing rate increased in coincidence with the flash intensity until the former got saturated. As expected, for every RGCs class (ON, OFF, and ON-OFF), the intensity-response curves of rd1 mice shifted to the right of WT controls, indicating a lower sensitivity to light (or a higher flash intensity needed to reach the half-maximum response). Treatment with LBP significantly shifted the curve back to the left for all RGC classes (Fig. 7B–E). There was a significant difference between LBP- and PBS-treated rd1 mice ($P < 0.001$ by one-way ANOVA with correction for repeated measures).

The calculated sensitivity (σ value = the intensity at which the response reaches the half maximum) measured by fitting the intensity profile with the Hill equation confirmed this result. A lower σ value indicates that a lower flash intensity is required to elicit a half-maximum response (i.e., the cell has a higher sensitivity). Treatment with LBP significantly increased the sensitivity of all rd1 RGCs. After combining RGCs from all three classes together, the σ for untreated RGCs was 8.9 ± 0.28 log photons/μm^2/s, while that for LBPs-treated was highly significantly lower at 7.2 ± 0.19 log photons/μm^2/s ($P < 0.001$ by one-way ANOVA; Fig. 7F). Interestingly, LBP treatment decreased the σ values only in the ON and the ON-OFF classes

Investigative Ophthalmology & Visual Science

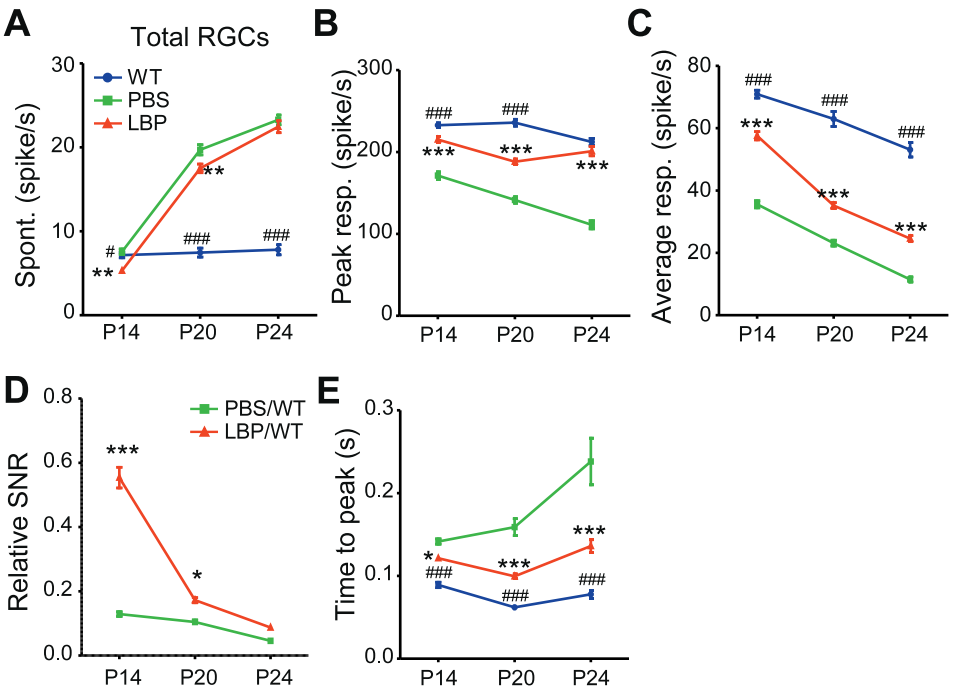

Figure 6. LBP treatment decreases the abnormally high spontaneous firing rate and increases the light response in the RGCs of rd1 mice. (**A**) Spontaneous firing rates of all recorded RGCs in different animal groups across ages. LBP treatment decreased the abnormally high spontaneous firing of rd1 RGCs at P14 and P20. (**B, C**) Peak responses (**B**) and average responses (**C**) over 2 seconds of light onset or offset in light-responsive cells of different animal groups. LBP treatment increased the light responses of rd1 cells. (**D**) SNRs of RGCs from PBS- or LBP-treated rd1 mice relative to those of WT counterparts. LBP treatment raised the relative SNR of rd1 RGCs at P14 and P20. (**E**) The time to peak light response of RGCs. LBP decreased the time to peak of rd1 RGCs. The light stimulus was a 2-second flash with an intensity of 3.6×10^7 photons/μm^2/s. The number of cells and animals recorded are the same as those in Fig. 5B. $^{*}P < 0.05$, $^{***}P < 0.001$ versus untreated mice; and $^{\#}P < 0.05$, $^{\#\#\#}P < 0.001$ versus LBP-treated rd1 mice by two-way ANOVA.

($P < 0.001$; Figs. 7G, 7H); in the OFF class the difference did not reach significance (Fig. 7I), possibly due to a smaller sample size for this group.

LBP Treatments Affects ON and OFF Pathways Differently

It has been shown that the ON and OFF pathways degenerate differently during photoreceptor degeneration,[36] we therefore wondered whether LBP has distinct effects on the ON and OFF pathways.

First, we compared the percentage of individual RGC classes (ON, ON-OFF, and OFF) relative to all the recorded (including responsive and nonresponsive) cells (Fig. 8). For all animal groups, the majority of the recorded cells were classified into the ON-OFF class, whereas the OFF cells were least recorded. For WT mice, the percentage of ON-OFF cells dropped while that of ON cells increased during development; this is consistent with the known developmental process of RGCs.[30] Compared with WT controls, the percentage of ON-OFF cells in untreated rd1 mice declined significantly over time, and LBP delayed their loss: at P14, this percentage was comparable among three animal groups; at P20, it dropped from 46% in WT to 27% in rd1 mice and LBP reversed it back to 40%; and at P24, the percentage reduced from 55% in WT to 11% in rd1 mice while LBP increased it to 39%. Similar phenomena were observed in ON cells, where the percentage of ON cells dropped from 43% and 37% in WT to 33% and 5% in rd1 mice at P20 and P24, respectively; LBP treatment in rd1 mice raised this percentage back to 39% and 16% at the corresponding time points. Because there were only a few OFF cells, differences in their percentages were marginal.

For each class, we subsequently compared the peak response of rd1 cells relative to that of WT controls at the same age (Figs. 9A–C). In rd1 retinas, the responses of the ON class deteriorated faster than those of the OFF cells. At P14, the ON responses of rd1 cells were only 55% of WT counterparts (Fig. 9A, green line), while those of OFF cells were 77% (Fig. 9C, green line). Later, the ON responses in rd1 retinas remained at around 57%, whereas the OFF responses dropped first to 46% at P20, and then to 38% at P24. The responses of the ON-OFF class in rd1 mice also decreased over time (Fig. 9B), and LBP treatment significantly enhanced their light responses at all ages tested, with a greater effect detected at P24. We did not observe a large effect of LBP on the OFF RGCs. Similar effects were also found when analyzing the relative mean responses of RGCs in rd1 retinas within 2 seconds of light onset or offset (rather than peak responses) (Supplemental Fig. 3). Notably, the mean responses of rd1 ON cells relative to WT counterparts were smaller than those of OFF cells at all ages. Again, LBP treatment increased the relative mean responses of both ON and ON-OFF cells in rd1 retinas.

To further quantify the protective effect of LBP on the light responses in individual RGC classes, we calculated the LBP/PBS ratio as the peak light responses in LBP-treated rd1 cells/light responses in PBS-treated rd1. Both the average ratio and the cumulative distribution showed a similar protective effect (1.2- to 1.4-fold of PBS group) for the three RGC classes at P14 (Fig. 9D). The greatest protection for ON and ON-OFF cells (relative to the other two classes) were observed at P20 (Fig. 9E) and P24 (Fig. 9F), respectively. Of note, the ratio of LBP/

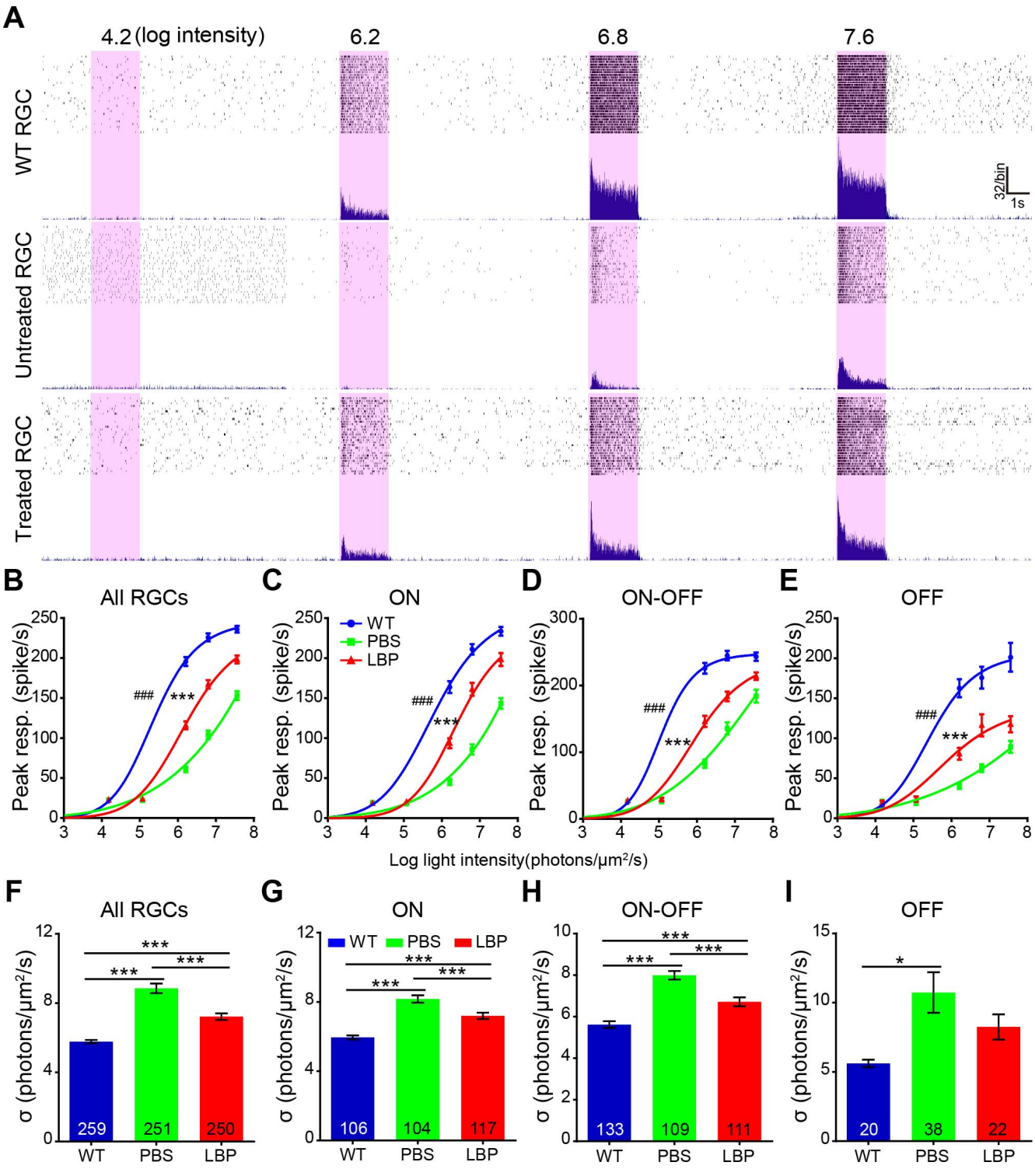

Figure 7. LBP treatment increases the light sensitivity of RGCs in rd1 mice at P20. (**A**) The raw record of a single RGC's responses to flashes with increasing intensities (the numbers indicate the flash intensity, with the unit in log photons/μm^2/s) from a WT, or an rd1 mouse receiving PBS or LBP administration. (**B–E**) Light intensity response curves of all (**B**), ON (**C**), ON-OFF (**D**), and OFF (**E**) RGCs for different animal groups, fitted with the Hill equation. The peak responses increased with light intensities. Generally, the light-evoked response of WT RGCs (*blue lines*) saturates at lower intensities than that of PBS-treated rd1 counterparts (*green lines*). The peak responses were much smaller in rd1 RGCs compared with WT controls at most flash intensities, while LBP treatment greatly improved the responses, thus shifting the curve to left. (**F–I**) Flash intensity required to reach the half-maximum response for all (**F**), ON (**G**), ON-OFF (**H**), and OFF (**I**) RGCs. The half-maximum flash intensity greatly increased in rd1 mice compared with WT controls, which was largely reversed by LBP treatment. The numbers within the *bars* represent the number of cells recorded. $^{*}P < 0.05$, $^{**}P < 0.01$, $^{***}P < 0.001$ versus untreated mice; and $^{\#\#}P < 0.05$, $^{\#\#\#}P < 0.001$, versus LBP-treated rd1 mice by one-way ANOVA for (**F–I**), or one-way ANOVA with corrections for repeated measures for (**B–E**).

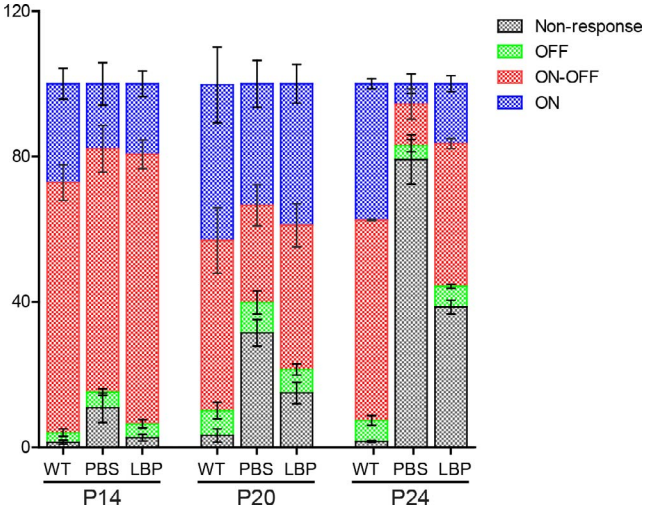

FIGURE 8. Changes of the percentage of three classes of RGCs and nonresponsive cells across ages. Percentages of ON (*blue*), ON-OFF (*red*), OFF (*green*), and nonresponsive RGCs (*gray*) of all recorded cells for different animal groups across ages. In rd1 mice, the percentage of ON-OFF and ON cells declined over time and remained lower than that in WT controls; LBP treatment delayed the above-mentioned cell losses. The numbers of cells and animals recorded are the same as those in Figure 5B. $^{**}P < 0.01$ for all cell classes at the same age by χ^2 analysis.

PBS for ON-OFF cells increased significantly from 1.23 ± 0.02 at P14 and 1.19 ± 0.03 at P20 to 1.97 ± 0.06 at P24 ($P < 0.001$ by one-way ANOVA), while for the other RGC classes the ratio remained consistent across ages ($P > 0.5$ for ON and OFF RGCs).

Having seen a large restoration by LBP in the ON-OFF RGCs, we wondered whether the ON and the OFF responses in these cells were equally recovered. The data demonstrated higher ratios of LBP/PBS in the ON responses at P14 ($P < 0.05$) and in the OFF responses at P24 ($P < 0.001$; Fig. 9G), indicating that for the ON-OFF RGCs, LBP protects the ON pathway to a greater extent at early stages, while protects the OFF pathway better at later stages. This finding was also favored by the cumulative distribution (Figs. 9H, 9I).

Discussion

In this study, we showed that LBP exerted protective effects on retinal neurons in rd1 mice. Morphologically, it increased the survival of photoreceptors and maintained the normal structures of cones and rod bipolar cells. Functionally, LBP treatment enhanced the responses of photoreceptors as well as RGCs, and improved animal visual behaviors. With regard to RGC responses in rd1 mice, LBP inhibited their abnormally high spontaneous firing and concurrently increased not only the responses to saturated light intensities, but also the light sensitivity as well as the SNR of the main three RGC classes. To the best of our knowledge, this is the first study that has examined in detail the effects of LBP on RGC responses.

LBP is a Promising Nutrient Able to Slow Down Photoreceptor Degeneration

LBP has proven effective for several retinal diseases in animal models, including ocular hypertension, optic nerve transection, ischemia, diabetic retinal neuropathy, and photoreceptor degeneration.[17–20,37,38] The protection is mostly attributed to its antioxidative, anti-inflammatory, and antiapoptotic properties.[20,38–42] However, it remains uncertain which component in LBP enables the aforementioned effects, despite L-arabinose seeming to partially account for the therapeutic effect in liver.[43]

In terms of retinal diseases, LBP has been studied for its impact on rd10 mouse retinas, where it slows down photoreceptor degeneration and improves visual behaviors.[20] Here, we demonstrated that LBP similarly decelerated photoreceptor degeneration in rd1 mice, a model exhibiting a faster degeneration compared with rd10 mice. The ability of LBP to prolong the function of a fast-degenerating circuit is supportive of its potential clinical applications to treat retinal diseases. Further, the data also lend support to a clinical trial aiming to rescue cone function in RP patients by use of extracts from wolfberry where LBP is the major ingredient (Registered Clinical Trial # NCT02244996, currently conducted by Hong Kong Polytechnic University, Hong Kong SAR, China). In fact, a 1-year follow-up has shown promising results where both ERG responses and visual acuity of RP patients have been significantly improved (Chan HHL, et al. *IOVS* 2016;57:ARVO E-Abstract 135). Only one patient exhibited a side effect of epistaxis (i.e., nose bleeding), and this is in contrast to prior studies where no severe side effects were reported when applying LBP to treat disorders, such as fatty liver disease,[43] brain ischemia,[44] and mood impairment.[45] Thus, the broad protective effects, low toxicity, and high availability of wolfberry enable LBP to serve as a promising constituent for RP treatment.

Differential Effects of LBP on ON and OFF Pathways During Photoreceptor Degeneration

Unlike in rd10 mice where rods may have residual light responses,[20,26] the mutated Pde6b enzyme loses expression and activity in rd1 mice,[46,47] so that all light responses are presumably generated by cones. However, the primary degeneration of rods leads to the secondary degeneration of cones, compromising the cone function over time. Accordingly, the preservation of light responses by LBP can be predominately attributed to deceleration of rod degeneration, which subsequently slows down cone degeneration. Notably, if cone integrity was the only difference between WT and rd1 retinas, we would expect both the ON and the OFF pathways to lose or gain activity at the same rate. Instead, we revealed that the rate of degeneration and the degree of protection changed over the course of development and degeneration. In particular, we found that LBP protected ON responses better than OFF responses at early stages of photoreceptor degeneration, whereas OFF responses were enhanced more than ON responses at later stages. The difference between ON and OFF responses may be accredited to LBP-elicited differential effects directly on ganglion cells. However, the density and morphology of ganglion cells do not change dramatically during the first 2 months of life in rd1 mice.[48–51] Hence, the functional and differential improvement is more likely due to differences in the first synaptic complex, as discussed below.

In the early stages of degeneration, we and others have noticed that ON responses deteriorate faster than OFF ones.[9,12,13] In rd10 mice, the metabotropic glutamate receptor 6 (mGluR6) on ON bipolar cells is lost before ionotropic glutamate receptors (iGluRs) on OFF bipolar cells.[12,52] In rd1 mice, poor functional activation of mGluR6 and aberrant iGluR activation in ON cone bipolar cells in the retina have been observed from P15.[53] This may explain the early loss in ON responses in this rd1 strain. With respect to the enhancement by LBP, we showed that it protected ON responses to a greater extent in the early stages of development, thus suggesting that LBP slows down not only cone degeneration, but also mGluR6

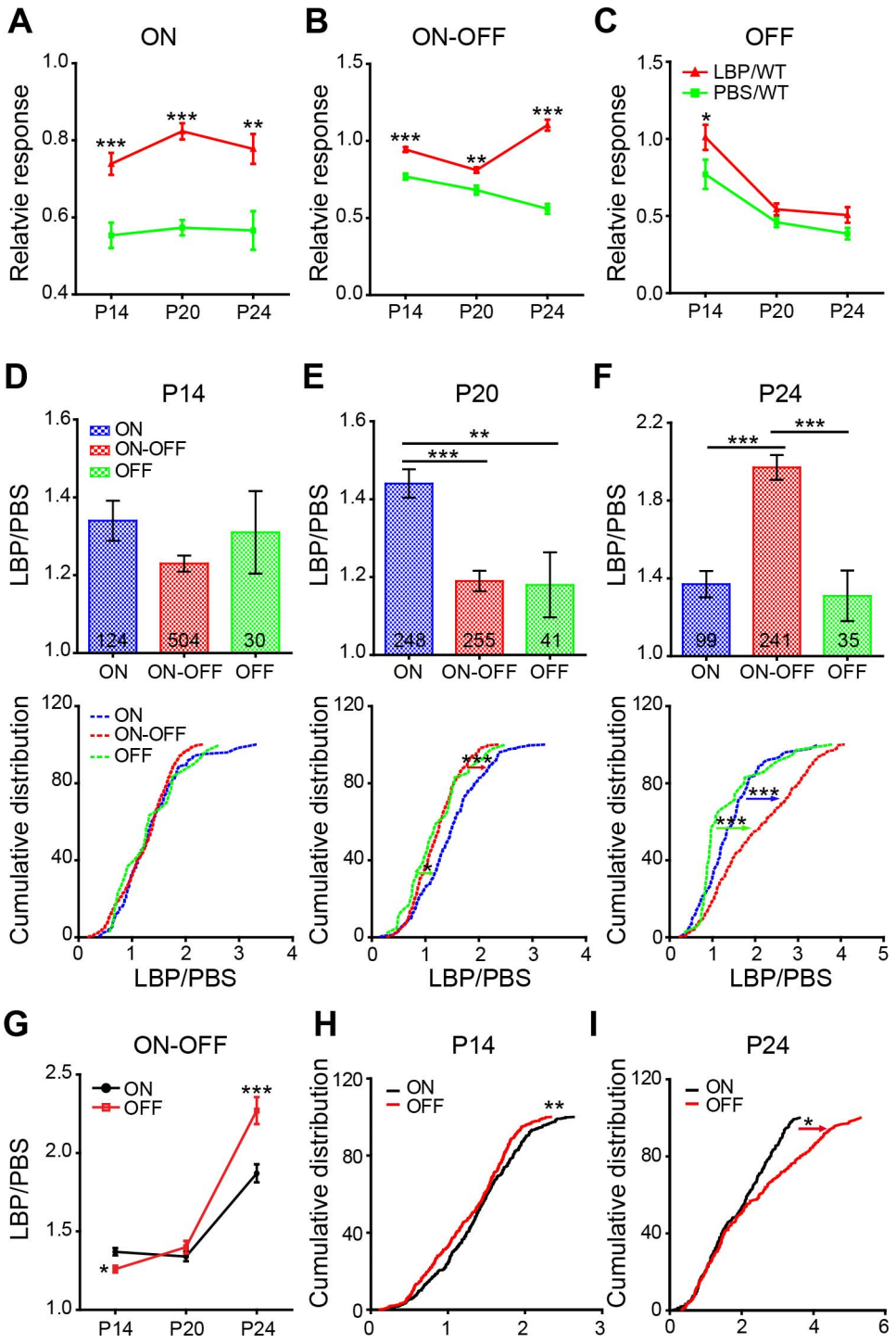

Figure 9. LBP treatment affects OFF and ON responses differently over time (**A**–**C**). Average peak responses of ON (**A**), ON-OFF (**B**), and OFF (**C**) RGCs in rd1 mice relative to those of WT controls across ages. LBP treatment significantly increased the relative peak responses of ON and ON-OFF, but not OFF cells (**D**–**F**). Average (*top trace*) and cumulative distribution (*low trace*) of the LBP/PBS ratio (peak light responses in LBP-treated rd1/light responses in PBS-treated rd1) for ON, ON-OFF, and OFF RGCs at P14 (**D**), P20 (**E**), and P24 (**F**). At P20, LBP showed a greater improvement (i.e., a larger LBP/PBS ratio) of light responses in ON RGCs than in ON-OFF and OFF cells, whereas at P24, LBP improved the light responses in ON-OFF RGCs to the greatest extent. (**G**) Ratios of LBP/PBS across ages for ON and OFF responses in ON-OFF RGCs. (**H**, **I**) Cumulative distribution of LBP/PBS ratios for ON and OFF responses in ON-OFF RGCs at P14 (**H**) and P24 (**I**). The numbers within the *bars* represent the number of cells recorded. $^{*}P < 0.05$, $^{**}P < 0.01$, $^{***}P < 0.001$ by two-way ANOVA or Kruskal-Wallis tests (for cumulative distribution curves).

loss. Another explanation may involve the modification of ectopic synapses formed between cones and rod bipolar cells in degenerated retinas.[54,55] Ectopic synapses have been shown to increase in rd1 mouse retinas.[54] If these synapses are further enhanced by LBP treatment, the cone signal to ON cells may increase via the following pathway: cones → rod bipolar cells (through ectopic synapses) → AII amacrine cells → ON cone bipolar cells (through gap junctions) → ON ganglion cells.

Another phenomenon observed in the early development of WT retinas is the reduced number of the ON-OFF class. This decline is probably owing to pruning, considering that RGCs initially stratify in both the ON and OFF sublaminas of the inner plexiform layer (IPL) and that they lose the diffuse stratification and some become monostratified during postnatal maturation.[30] In our study, we noticed that the loss of ON-OFF RGCs in rd1 retinas was much faster than in WT counterparts, which is potentially due to the faster loss of ON responses, so that even a bistratified RGC could only respond to an OFF stimulus. Our finding that LBP treatment improved ON-OFF responses at P14 and P20 can therefore be explained by its preservation of ON responses.

At later stages of degeneration, ON responses continued to deteriorate. While LBP continued to protect the ON pathway, such a protective effect seemed to target the ON-OFF class (Figs. 9B, 9D). During these stages, when separating ON response from OFF response in the ON-OFF population, improvement of the OFF response was greater than that of the ON response. In both rd10 and rd1 retinas, iGluR expression in the dendrites of OFF bipolar cells increases.[12,56] Accordingly, provided that the expression of iGluRs has increased even more in LBP-treated rd1 retinas, we would expect a greater enhancement for OFF responses. Another interesting finding is that although OFF responses were improved in both OFF and ON-OFF RGCs, those in ON-OFF cells seemed greater. Given that alterations to the ON-OFF class require changes of transmission in the IPL, it is possible that LBP slowed down the physiological conversion from multistratified to monostratified cells due to interruptions within developmental processes, subsequently increasing the ON-OFF population to a greater extent than other classes. Indeed, the change in stratification of RGCs in the rd1 retina has been documented.[57] Another possibility is that there may be a specific modulation of iGluRs on ON-OFF cells. In cultured cortical neurons, LBP increased the expression of N-methyl-D-aspartate (NMDA) receptor subunit NR2A while inhibited that of NR2B,[44] leading to a neuroprotective effect in the ischemic injury. In the retina, NMDA receptors are known to be expressed on RGCs with different distributions in varied classes.[58–60] Furthermore, during development, both NR2A and NR2B receptors are expressed on several RGC classes and regulate their development and maturity.[60] In the adult retina, NR2B is downregulated, while NR2A remains dominant. Therefore, the dysregulation of NR2B in the rd1 retina may be attributed to its reduced activity; LBP restores this regulation, and thereby alters the intensities of ON and OFF responses differentially.

In conclusion, in a photoreceptor fast-degenerating mouse model (rd1), LBP greatly improves visual processing at multiple stages of information transmission. This involves a series of protections on: (1) the morphology of photoreceptors (including rods, cones, and their terminals) and rod bipolar cells at the first and the second stages of visual processing, respectively; (2) the function of the above-mentioned cell types, as evidenced by their ERG responses; (3) the function of RGCs at the third stage of visual processing, as assessed by MEA recording; and (4) perhaps the function of higher brain centers as suggested by enhanced visual behavior. Therefore, the multifaceted protections offered by LBP may extend the time window for RP treatment with more invasive approaches, such as retinoprosthesis.

Acknowledgments

The authors thank Hui Chen for technical help with MEA recording, and Ang Li and Tamar Vardi for proofreading this manuscript.

Supported by grants from the National Natural Science Foundation of China (81470656; Beijing, China); Ningxia Key Research and Development Program Grant (Yinchuan, Ningxia, China); the 111 Project, Ministry of Education and State Administration of Foreign Experts Affairs of PRC (B14036; Beijing, China); and the Science & Technology Planning and Key Technology Innovation Projects of Guangdong (2014B050504006; Guangzhou, Guangdong, China).

Disclosure: **F. Liu**, None; **J. Zhang**, None; **Z. Xiang**, None; **D. Xu**, None; **K.-F. So**, None; **N. Vardi**, None; **Y. Xu**, None

References

1. Hartong DT, Berson EL, Dryja TP. Retinitis pigmentosa. *Lancet*. 2006;368:1795–1809.
2. Wang J, Saul A, Roon P, Smith SB. Activation of the molecular chaperone, sigma 1 receptor, preserves cone function in a murine model of inherited retinal degeneration. *Proc Natl Acad Sci U S A*. 2016;113:E3764–E3772.
3. Bennett J, Tanabe T, Sun D, et al. Photoreceptor cell rescue in retinal degeneration (rd) mice by in vivo gene therapy. *Nat Med*. 1996;2:649–654.
4. Komeima K, Rogers BS, Lu L, Campochiaro PA. Antioxidants reduce cone cell death in a model of retinitis pigmentosa. *Proc Natl Acad Sci U S A*. 2006;103:11300–11305.
5. MacLaren RE, Pearson RA, MacNeil A, et al. Retinal repair by transplantation of photoreceptor precursors. *Nature*. 2006; 444:203–207.
6. Yue L, Weiland JD, Roska B, Humayun MS. Retinal stimulation strategies to restore vision: fundamentals and systems. *Prog Retin Eye Res*. 2016;53:21–47.
7. Bi A, Cui J, Ma YP, et al. Ectopic expression of a microbial-type rhodopsin restores visual responses in mice with photoreceptor degeneration. *Neuron*. 2006;50:23–33.
8. Margolis DJ, Newkirk G, Euler T, Detwiler PB. Functional stability of retinal ganglion cells after degeneration-induced changes in synaptic input. *J Neurosci*. 2008;28:6526–6536.
9. Stasheff SF. Emergence of sustained spontaneous hyperactivity and temporary preservation of OFF responses in ganglion cells of the retinal degeneration (rd1) mouse. *J Neurophysiol*. 2008;99:1408–1421.
10. An GJ, Asayama N, Humayun MS, et al. Ganglion cell responses to retinal light stimulation in the absence of photoreceptor outer segments from retinal degenerate rodents. *Curr Eye Res*. 2002;24:26–32.
11. Pu M, Xu L, Zhang H. Visual response properties of retinal ganglion cells in the Royal College of Surgeons dystrophic rat. *Invest Ophthalmol Vis Sci*. 2006;47:3579–3585.
12. Puthussery T, Gayet-Primo J, Pandey S, Duvoisin RM, Taylor WR. Differential loss and preservation of glutamate receptor function in bipolar cells in the rd10 mouse model of retinitis pigmentosa. *Eur J Neurosci*. 2009;29:1533–1542.
13. Fransen JW, Pangeni G, Pyle IS, McCall MA. Functional changes in Tg P23H-1 rat retinal responses: differences between ON and OFF pathway transmission to the superior colliculus. *J Neurophysiol*. 2015;114:2368–2375.
14. Yee CW, Toychiev AH, Sagdullaev BT. Network deficiency exacerbates impairment in a mouse model of retinal degeneration. *Front Syst Neurosci*. 2012;6:8.
15. Sekirnjak C, Hottowy P, Sher A, Dabrowski W, Litke AM, Chichilnisky EJ. Electrical stimulation of mammalian retinal ganglion cells with multielectrode arrays. *J Neurophysiol*. 2006;95:3311–3327.
16. Farah N, Reutsky I, Shoham S. Patterned optical activation of retinal ganglion cells. *Conf Proc IEEE Eng Med Biol Soc*. 2007;2007:6368–6370.
17. Chu PH, Li HY, Chin MP, So KF, Chan HH. Effect of lycium barbarum (wolfberry) polysaccharides on preserving retinal

function after partial optic nerve transection. *PLoS One*. 2013;8:e81339.

18. Li SY, Yang D, Yeung CM, et al. Lycium barbarum polysaccharides reduce neuronal damage, blood-retinal barrier disruption and oxidative stress in retinal ischemia/reperfusion injury. *PLoS One*. 2011;6:e16380.
19. Mi XS, Feng Q, Lo AC, et al. Protection of retinal ganglion cells and retinal vasculature by Lycium barbarum polysaccharides in a mouse model of acute ocular hypertension. *PLoS One*. 2012;7:e45469.
20. Wang K, Xiao J, Peng B, et al. Retinal structure and function preservation by polysaccharides of wolfberry in a mouse model of retinal degeneration. *Sci Rep*. 2014;4:7601.
21. Chan HC, Chang RC, Koon-Ching Ip A, et al. Neuroprotective effects of Lycium barbarum Lynn on protecting retinal ganglion cells in an ocular hypertension model of glaucoma. *Exp Neurol*. 2007;203:269–273.
22. Jia X, Liong EC, Ching YP, et al. Lycium barbarum polysaccharides protect mice liver from carbon tetrachloride-induced oxidative stress and necroinflammation. *J Ethnopharmacol*. 2012;139:462–470.
23. Strettoi E, Porciatti V, Falsini B, Pignatelli V, Rossi C. Morphological and functional abnormalities in the inner retina of the rd/rd mouse. *J Neurosci*. 2002;22:5492–5504.
24. Lin B, Koizumi A, Tanaka N, Panda S, Masland RH. Restoration of visual function in retinal degeneration mice by ectopic expression of melanopsin. *Proc Natl Acad Sci U S A*. 2008;105:16009.
25. Frankfort BJ, Khan AK, Tse DY, et al. Elevated intraocular pressure causes inner retinal dysfunction before cell loss in a mouse model of experimental glaucoma. *Invest Ophthalmol Vis Sci*. 2013;54:762–770.
26. Zhang J, Xu D, Ouyang H, et al. Neuroprotective effects of methyl 3,4 dihydroxybenzoate in a mouse model of retinitis pigmentosa. *Exp Eye Res*. 2017;162:86–96.
27. Yang S, Luo X, Xiong G, So KF, Yang H, Xu Y. The electroretinogram of Mongolian gerbil (Meriones unguiculatus): comparison to mouse. *Neurosci Lett*. 2015;589:7.
28. Segev R, Goodhouse J, Puchalla J, Berry MJ. Recording spikes from a large fraction of the ganglion cells in a retinal patch. *Nat Neurosci*. 2004;7:1154–1161.
29. Chen H, Liu X, Tian N. Subtype-dependent postnatal development of direction- and orientation-selective retinal ganglion cells in mice. *J Neurophysiol*. 2014;112:2092–2101.
30. Tian N, Copenhagen DR. Visual stimulation is required for refinement of ON and OFF pathways in postnatal retina. *Neuron*. 2003;39:85–96.
31. Pu M, Xu L, Zhang H. Visual response properties of retinal ganglion cells in the royal college of surgeons dystrophic rat. *Invest Ophthalmol Vis Sci*. 2006;47:3579–3585.
32. Sampath AP, Rieke F. Selective transmission of single photon responses by saturation at the rod-to-rod bipolar synapse. *Neuron*. 2004;41:431–443.
33. Carter-Dawson LD, Lavail MM, Sidman RL. Differential effect of the rd mutation on rods and cones in the mouse retina. *Invest Ophthalmol Vis Sci*. 1978;17:489–498.
34. Blanks JC, Adinolfi AM, Lolley RN. Photoreceptor degeneration and synaptogenesis in retinal-degenerative (rd) mice. *J Comp Neurol*. 1974;156:95.
35. Yong SG, Park DJ, Ahn JR, Senok SS. Spontaneous oscillatory rhythms in the degenerating mouse retina modulate retinal ganglion cell responses to electrical stimulation. *Front Cellular Neurosci*. 2016;9:512.
36. Stasheff S. Emergence of sustained spontaneous hyperactivity and temporary preservation of OFF responses in ganglion cells of the retinal degeneration (rd1) mouse. *J Neurophysiol*. 2008;99:1408–1421.
37. Guo J, Xu GX, Hou ZJ, Xu JB, Huang LY. Effect of Lycium barbarum polysaccharides on the retinal ultrastructure of streptozocin-induced diabetic rats [in Chinese]. *Zhongguo Zhong Xi Yi Jie He Za Zhi*. 2013;33:1404–1407.
38. Zhu Y, Zhao Q, Gao H, Peng X, Wen Y, Dai G. Lycium barbarum polysaccharides attenuates N-methy-N-nitrosourea-induced photoreceptor cell apoptosis in rats through regulation of poly (ADP-ribose) polymerase and caspase expression. *J Ethnopharmacol*. 2016;191:125–134.
39. Chiu K, Chan HC, Yeung SC, et al. Modulation of microglia by Wolfberry on the survival of retinal ganglion cells in a rat ocular hypertension model. *J Ocul Biol Dis Inform*. 2009;2:47–56.
40. He M, Pan H, Chang RC, So KF, Brecha NC, Pu M. Activation of the Nrf2/HO-1 antioxidant pathway contributes to the protective effects of Lycium barbarum polysaccharides in the rodent retina after ischemia-reperfusion-induced damage. *PLoS One*. 2014;9:e84800.
41. Li H, Liang Y, Chiu K, et al. Lycium barbarum (wolfberry) reduces secondary degeneration and oxidative stress, and inhibits JNK pathway in retina after partial optic nerve transection. *PLoS One*. 2013;8:e68881.
42. Yang D, So KF, Lo AC. Lycium barbarum polysaccharides extracts preserve retinal function and attenuate inner retinal neuronal damage in a mouse model of transient retinal ischemia. *Clin Exp Ophthalmol*. 2017;45:717–729.
43. Xiao J, Xing F, Huo J, et al. Lycium barbarum polysaccharides therapeutically improve hepatic functions in non-alcoholic steatohepatitis rats and cellular steatosis model. *Sci Rep*. 2014;4:5587.
44. Shi Z, Zhu L, Li T, et al. Neuroprotective mechanisms of Lycium Barbarum polysaccharides against ischemic insults by regulating NR2B and NR2A containing NMDA receptor signaling pathways. *Front Cell Neurosci*. 2017;11:288.
45. Po KK, Leung JW, Chan JN, et al. Protective effect of Lycium Barbarum polysaccharides on dextromethorphan-induced mood impairment and neurogenesis suppression. *Brain Res Bull*. 2017;134:10–17.
46. Chang B, Hawes NL, Pardue MT, et al. Two mouse retinal degenerations caused by missense mutations in the beta-subunit of rod cGMP phosphodiesterase gene. *Vision Res*. 2007;47:624–633.
47. Farber DB, Lolley RN. Enzymic basis for cyclic GMP accumulation in degenerative photoreceptor cells of mouse retina. *J Cyclic Nucleotide Res*. 1976;2:139–148.
48. Lin B, Peng EB. Retinal ganglion cells are resistant to photoreceptor loss in retinal degeneration. *PLoS One*. 2013;8:e68084.
49. Anderson EE, Greferath U, Fletcher EL. Changes in morphology of retinal ganglion cells with eccentricity in retinal degeneration. *Cell Tissue Res*. 2016;364:263–271.
50. Saha S, Greferath U, Vessey KA, Grayden DB, Burkitt AN, Fletcher EL. Changes in ganglion cells during retinal degeneration. *Neuroscience*. 2016;329:1–11.
51. Damiani D, Novelli E, Mazzoni F, Strettoi E. Undersized dendritic arborizations in retinal ganglion cells of the rd1 mutant mouse: a paradigm of early onset photoreceptor degeneration. *J Comp Neurol*. 2012;520:1406–1423.
52. Gayet-Primo J, Puthussery T. Alterations in Kainate Receptor and TRPM1 localization in bipolar cells after retinal photoreceptor degeneration. *Front Cell Neurosci*. 2015;9:486.
53. Chua J, Fletcher EL, Kalloniatis M. Functional remodeling of glutamate receptors by inner retinal neurons occurs from an early stage of retinal degeneration. *J Comp Neurol*. 2009;514:473–491.
54. Peng YW, Hao Y, Petters RM, Wong F. Ectopic synaptogenesis in the mammalian retina caused by rod photoreceptor-specific mutations. *Nat Neurosci*. 2000;3:1121–1127.

Investigative Ophthalmology & Visual Science

55. Peng YW, Senda T, Hao Y, Matsuno K, Wong F. Ectopic synaptogenesis during retinal degeneration in the royal college of surgeons rat. *Neuroscience*. 2003;119:813–820.
56. Srivastava P, Sinha-Mahapatra SK, Ghosh A, Srivastava I, Dhingra NK. Differential alterations in the expression of neurotransmitter receptors in inner retina following loss of photoreceptors in rd1 mouse. *PLoS One*. 2015;10:e0123896.
57. O'Brien EE, Greferath U, Fletcher EL. The effect of photoreceptor degeneration on ganglion cell morphology. *J Comp Neurol*. 2014;522:1155–1170.
58. Fletcher EL, Hack I, Brandstatter JH, Wassle H. Synaptic localization of NMDA receptor subunits in the rat retina. *J Comp Neurol*. 2000;420:98–112.
59. Zhang J, Diamond JS. Subunit- and pathway-specific localization of NMDA receptors and scaffolding proteins at ganglion cell synapses in rat retina. *J Neurosci*. 2009;29:4274–4286.
60. Stafford BK, Park SJ, Wong KY, Demb JB. Developmental changes in NMDA receptor subunit composition at ON and OFF bipolar cell synapses onto direction-selective retinal ganglion cells. *J Neurosci*. 2014;34:1942–1948.

Investigative Ophthalmology & Visual Science